Sensors & Transducers, Vol. 218, Issue 12, December 2017, pp. 40-48

www.sensorsportal.com

Sensors & Transducers

Published by IFSA Publishing, S. L., 2017
http://www.sensorsportal.com

Vehicle-to-Vehicle and Infrastructure-to-Vehicle Communication in the Visible Range

[1, 2] M. A. Vieira, [1, 2, 3] M. Vieira, [1, 3] P. Vieira and [1, 2] P. Louro

[1] ADETC/ISEL/IPL, R. Conselheiro Emídio Navarro, 1959-007 Lisboa, Portugal
[2] CTS-UNINOVA Quinta da Torre, Monte da Caparica, 2829-516, Caparica, Portugal
[3] DEE-FCT-UNL Quinta da Torre, Monte da Caparica, 2829-516, Caparica, Portugal
[4] Instituto das Telecomunicações, Instituto Superior Técnico, 1049-001, Lisboa, Portugal
[1] Tel.: +351218317000, fax: +351218317114
E-mail: mv@isel.ipl.pt

Received: 10 November 2017 /Accepted: 10 December 2017 /Published: 29 December 2017

Abstract: This paper proposes the use of Visible Light Communication (VLC) for vehicle safety applications, creating a smart vehicle lighting system that combines the functions of illumination and signalling, communications, and positioning. The feasibility of VLC is demonstrated by employing trichromatic Red-Green-Blue (RGB) LEDs as transmitters, since they offer the possibility of Wavelength Division Multiplexing (WDM), which can greatly increase the transmission data rate, when using SiC double p-i-n receivers to encode/decode the information. Each chip, individually, is used to transmit the driving range distance and data information. An on-off code is used to transmit the data. Free space is the transmission medium. The receivers consist of two stacked amorphous a-H:SiC cells. Multiple Input Multiple Output (MIMO) architecture is used. For data transmission, Streetlights and headlights based on commercially available modulated white RGB-LEDs are used. For data receiving and decoding, three a-SiC:H double pin/pin optical processors symmetrically distributed at the vehicle tail are utilized. The process of accurately encoding and decoding positioning and the design of SiC navigation system are discussed and tested. A visible multilateration method estimates the drive distance range. Infrastructure-to-Vehicle (I2V) and Vehicle-to-Vehicle (V2V) Communication are simulated.

Keywords: a-SiC:H technology, LED, Visible Light Communication, Intelligent Transportation System, Optical sensor, WDM, Vehicular Communication.

1. Introduction

Modern vehicles are equipped with many electronic sensors which monitor a vehicle's speed, position, heading, and lateral and longitudinal acceleration. Although the technology exists to do so, vehicles rarely communicate this information wirelessly to other vehicles or roadside infrastructure. Researchers are anticipating the deployment of wireless vehicle communication, and have begun developing applications that use this new technology to improve safety and reduce congestion. This system is known as connected vehicles.

Recently, the demand for the solution of road traffic problems such as accidents, congestion and the associated environmental pollution, has significantly increased. By enabling wireless communication among vehicles and between vehicles and infrastructure, the safety and the efficiency of road traffic can be substantially improved. Until recently, vehicles were unable to share their data in any meaningful way. Vehicle-to-vehicle (V2V)

communication was limited to brake lights, turn signals, and other low-tech methods**.** Infrastructure-to-vehicle (I2V) communication was likewise limited to dynamic message signs, highway advisory radio, traffic signals, and ramp meters.

Several modes of vehicular communications, such as infrastructure-to-vehicle (I2V), vehicle-to-vehicle (V2V) and vehicle-to-infrastructure (V2I) are becoming increasingly popular, boosted by navigation safety requirements [1].

Current solutions, such as intelligent traffic control systems, provide communication infrastructures along the road; vehicular communication and likewise, are research trends under the area of Intelligent Transportation Systems (ITS) [2-4].

Recently, LED-based optical wireless communication has been also proposed for car to car message delivery. This option turned out to be particularly effective in short range direct communications to explore Line-of-Sight (LoS) and overcome the issues related to the isotropic nature of radio waves. One additional benefit of LEDs is that they can switch to different light intensities at a very fast rate. This functionality has given rise to a novel communication technology (Visible Light Communication - VLC) where LED luminaires can be used for high speed data transfer [5-6].

In the recent past, we have developed a WDM device that enhances the transmission capacity of optical communications in the visible range. When different visible signals are encoded in the same optical transmission path [7-8] the device multiplexes the different optical channels, performs different filtering processes (amplification, switching, and wavelength conversion) and finally decodes the encoded signals recovering the transmitted information. This device is used as a receiver. Therefore, by utilizing VLC between vehicles, drivers are given a clearer knowledge of the preceding and nearby vehicles status.

In this paper, a traffic scenario is established. The transmitters and the receivers are characterized. To achieve vehicular communication (V2V) 4 bit string color messages in the visible range and their three parity bits for error control are used to transmit a codeword that is received and decoded by the SiC pinpin devices. Code and parity multiplex/demultiplex (MUX/DEMUX) signals are designed, transmitted and analyzed. The dependence of distance between the transmitter and receiver on the shape and magnitude of the encoded signal is presented. Driving range distance is discussed and tested using the VLC system. The proposed smart vehicle lighting system considers wireless communication, computer based algorithms and smart sensor and optical sources network, which builds a transdisciplinary approach framed in cyber-physical systems.

This paper is organized as follows. In Section 1, the introduction is present and in Section 2, the system design is explained. Section 3, reports the encoder/decoder method and in Section 4, the driving distance is analyzed. In section 5, an example of I2V follow by V2V communication is presented. Finally, in Section 6, conclusions are drawn.

2. System Design

2.1. The Traffic Scenario

White RGB-LEDs using WDM can achieve higher data transfer rates and can also be used for lighting purposes [9]. For data transmission, we propose the use of two headlights based on commercially available modulated white RGB-LEDs. For data receiving and decoding, three a-SiC:H double pin/pin optical processors symmetrically distributed at the vehicle tail are used (see Fig. 1).

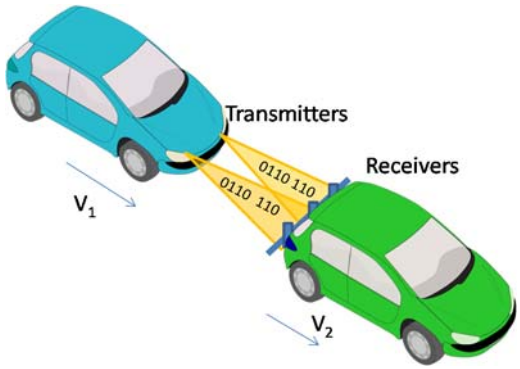

Fig. 1. Illustration of the V2V. Use Case: the follower vehicle sends the message that is received by the leader and can be retransmitted for the next car.

This VLC system enables the data transmission between vehicles, which is crucial to stack the information concerning the status of the vehicle (e.g., brake, speed, acceleration, engine failure, traffic congestion). To build a one-way VLC system that allows a feedback channel between the leader vehicle and the follower vehicle, the follower vehicle is assumed equipped with two headlamps transmitters. They send a codeword message [RGBV: P_R, P_G, P_B] composed of red, green, blue and violet 4-binary bits (four input data bits [R G B V]) and generate three additional parity bits [P_R, P_G, P_B] for easy decoding and error control [10]. The parity bits are SUM bits of the three-bit additions of violet pulsed signal, with two additional bits of RGB. The leader vehicle is assumed to be equipped with three a-SiC pinpin receivers to detect optical messages, as in Fig. 1. The spacing of the two transmitters is fixed while their distance to the receivers varies and depends on the speed (v_1, v_2). Both transmitters are oriented towards the receivers. In Fig. 2, the geometrical relation between the two vehicles (leader vehicle and follower vehicle) and the separating distances (A, B and C) are displayed. Here, the follower vehicle sends the

information using the modulated light from the headlamps forming a lighting coverage. The leader vehicle receives and decodes the message in three separated receivers at the tail and compares them. It was assumed that each LED chip sends light only perpendicular to the semiconductor's surface, and a few degrees to the side, which results in a light cone pattern (Fig. 2). Three situations are possible: A, the vehicles are at a safety distance and the three sensors receive the same message with the same intensity; B, the vehicles are in a warning distance, they are approaching and the left and the right sensor receive the same message but at the middle sensor the message arrives with double intensity; C the vehicles are too close, in the automatic braking distance, and the same message arrives to the left and to the right sensor and no message is read out by the middle one. Based on that, the driving range distance is calculated and a warning is sent to the driver or eventually activates the automatic braking system.

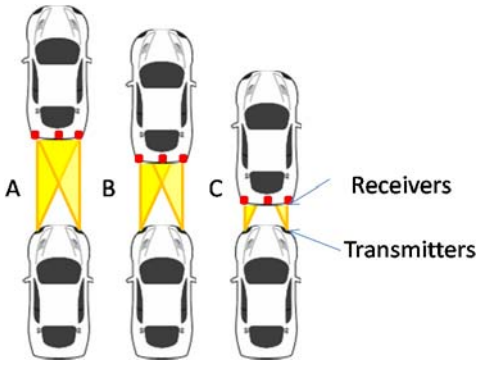

Fig. 2. Driving range distance showing the inter-vehicle distance decreasing as total photocurrent on the three receivers changes.

2.2. Transmitters

The usage of trichromatic RGB-LEDs as transmitters offers the possibility of WDM which can greatly increase the transmission data rate. For data transmission, we use commercially available violet and white RGB-LEDs whose spectra is displayed in Fig. 3.

The output spectra of the white LED contains three peaks assigned to the colors red, green and blue that mixed together provide the white perception to the eye. They are used for lighting purposes and when modulated, to transmit data. Each chip, in the trichromatic LED, can be switched *on* and *off* individually for a desired bit sequence [R G B]. An extra violet modulated LED [V] was added to increase data transmission and to generate parity bits [11] that allow error control [12].

In Table 1 the optical characteristics of the white LEDs at 25 ºC are reported.

For data transmission, an on-off keying (OOK) code was used. In Fig. 4, an example of the digital signals (codeword) used to drive the LEDs is displayed.

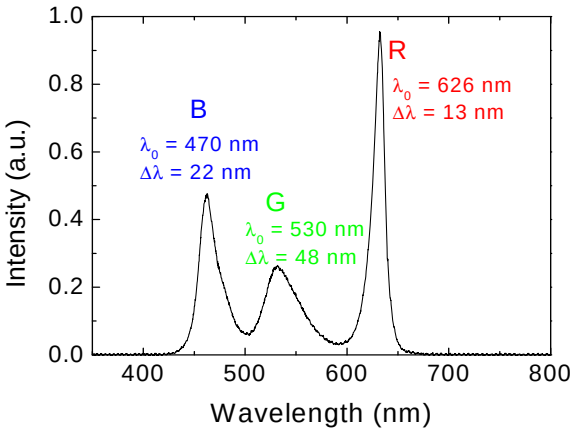

Fig. 3. Normalized emission spectra for the white RGB-LED.

Table 1. White LEDs characteristics at 25 ºC.

	Red (R)	Green (G)	Blue (B)
Dominant wavelength (nm)	619 - 624	520 - 540	460 - 480
Luminous intensity (mcd)	355 - 900	560 - 1400	180 - 505
Spectral bandwidth @ 20 mA	24	38	28

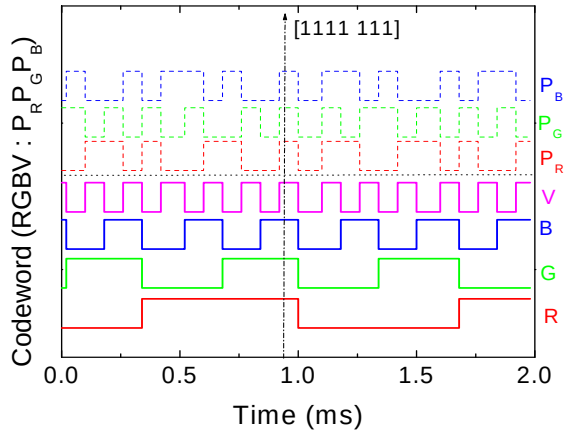

Fig. 4. Representation of the original encoded message [R G B V; P_R P_G P_B].

All the sixteen (2^4) *on/off* possible combinations of the 4 input channels (RGBV) are reported as well the corresponding parity bits. The arrow sets the seven bit [1111:111] codeword. Here, the Hamming (7,4) code [11] encodes the 4 bits (four input channels, RGBV) of data into 7 bits by adding 3 parity bits. The encoder takes four input data bits [R G B V] to which corresponds one of the possible 16 combinations and generates three additional parity bits, i.e., the parity bits are SUM bits of the three-bit additions of violet pulsed signal with two additional bits of RGB [12] and are given by:

$$P_R\text{-}(VRB) = V \oplus R \oplus B, \quad (1)$$

$$P_G\text{-}(VRG) = V \oplus R \oplus G, \quad (2)$$

$$P_B\text{-}(VGB) = V \oplus G \oplus B \quad (3)$$

Moreover, the seven-bit codeword at the output of the encoder will be in a format, with the data and the parity bits [R G B V; P_R P_G P_B] separated.

2.3. Receiver

The optoelectronic sensor is a double pin heterostructure produced by Plasma Enhanced Chemical Vapor Deposition (PECVD) sandwiched between two transparent conductive contacts (TCO). The device configuration is shown in Fig. 5. In the stacked structure, p-i'(a-SiC:H)-n/p-i(a-Si:H)-n, the intrinsic layer of the front p-i-n photodiode in made of a-SiC:H while the back intrinsic layer is based on a-Si:H. The deposition conditions and optoelectronic characterization of the single layers and device as well as their optimization were described in [7] and [8]. Both front and back diodes act as optical filters confining, respectively, the optical carriers produced by the blue and red photons, while the optical carriers generated by the green photons are absorbed across both.

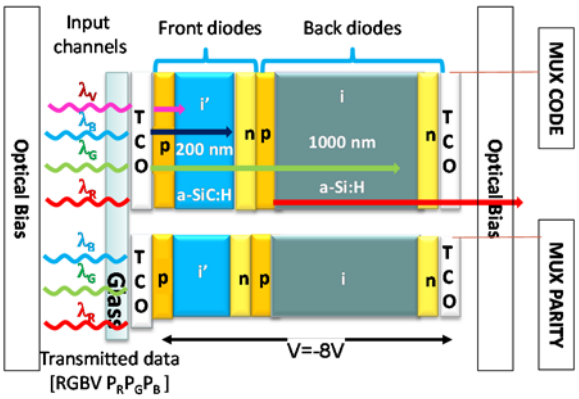

Fig. 5. Receiver configuration and operation.

A polychromatic mixture of red, green, blue and violet; $\lambda_{R,G,B,V;}$ pulsed communication channels (input channels; transmitted data) are combined together, each one with a specific bit sequence and absorbed according to their wavelengths (see arrow magnitudes in Fig. 5). The combined optical signal (multiplexed signal; received data) is analyzed by reading out the generated photocurrent under negative applied voltage (-8 V), with and without 390 nm background lighting, applied either from front or back sides [13]. The RGB-LEDs are used together for illumination purposes and individually to transmit the channel location and data information.

2.4. Optical Filter

Four monochromatic input channels illuminated the device separately (transmitted data) or combined (MUX signal) with 12 kbps transmission rate. The generated photocurrent was measured. For the red and violet channels, the photocurrents without optical bias (no bias) and under front and back lighting are displayed in Fig. 6. Results show that front irradiation enhances the red signal and decreases the violet, while back irradiation has the opposite effect (see arrows in the figure).

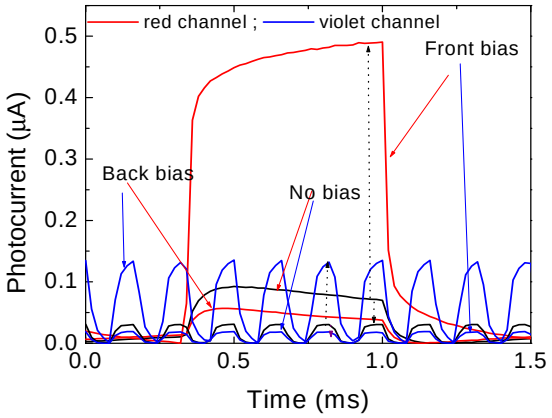

Fig. 6. Red and violet signals without (No bias) and under front (Front bias) and back (Back bias) irradiation.

The gathered data confirms that the optical gain, under irradiation, depends on the irradiated side and on the incoming wavelength acting as an active filter for the input channels [13]. Under front irradiation, the long wavelength channels are enhanced and the short wavelength channels quenched while the opposite occurs under back irradiation.

3. Encoder / Decoder

The algorithm to decode the information is relatively straightforward and the knowledge of the background acting as selector that chooses one or more of the 2^n sublevels (with *n* being the number of transmitted channels) and their *n*-bit binary code makes the communication reliable [14].

In Fig. 7, the received data, i.e., the MUX code signal, due to the combination of four (400 nm, 470 nm, 530 nm, 626 nm) input channels and the correspondent parity bits are displayed under front irradiation. The solid lines show the MUX signal that arises from the transmission of the four (R, G, B, V) wavelength channels. The dashed line marks the synchronized parity MUX signal transmitted with the data code. Due to the different optical gains, the colors red, green and blue were assigned respectively to the transmission of P_R, P_G and P_B.

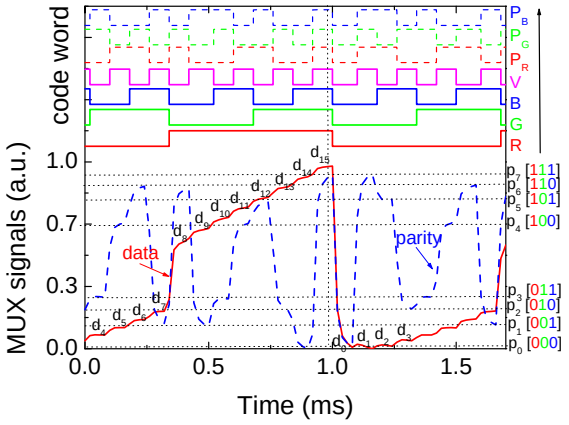

Fig. 7. Code and parity MUX/DEMUX signals under 390 nm front irradiation. On the top the transmitted channels [R G B V: P_R P_G P_B] are decoded.

The sixteen ordered levels (d_0-d_{15}) of the data MUX signal are pointed out at the correspondent levels, and the ordered eight levels (p_0-p_7) ascribed to the parity bits are displayed as horizontal dotted lines. On the right hand side of Fig. 7, the correspondence between the parity levels and the parity bits is shown. In the top, the decoded seven bit word [R, G, B,V, P_R, P_G, P_B] of the transmitted inputs is displayed. Results show that each of the 2^n possible *on/off* states corresponds to a well-defined level. In Fig. 7, all the *on/off* states are possible hence, 2^4 ordered levels are detected (d_0-d_{15}) and correspond to all the possible combinations of the *on/off* states. Under front irradiation, each of those *n* channels is enhanced or quenched differently, resulting in an increase of red/green magnitude and a decrease on the blue/violet magnitude. In the sequence, by assigning each output level to a *n* digit binary code (weighted by the optical gain of the each channel), the signal can be decoded. A maximum transmission rate capability of 30 kbps was achieved in a four channel transmission.

The proximity of the magnitude of consecutive levels (Fig. 7) causes occasional errors in the decoded information that is corrected using the parity bits. For instance, levels d_1, d_2, and d_3 have similar magnitude and can be confused when reading a word message, however their parity levels, respectively, p_7, p_5 and p_2, are quite different. The parity of the word is checked after reading the word. The word is accepted if the parity of the bits read out is correct. If the parity of the bits is incorrect, an error is detected and should be corrected [12].

To automate the process of recovering the original transmitted data, an enhanced algorithm was developed. The transmitted information is decoded by comparing both the signal from the code and parity MUX levels under front irradiation, as shown in Fig. 7. The decoding algorithm is based on a proximity search [15]. The vector components are determined by the signal currents I_1 and I_2, where I_1 (d levels) and I_2 (p levels) are the currents measured simultaneously, under front optical bias, for the 4-bit codeword (RGBV) and for the 3-bit parity [P_R, P_G P_B]. The result is then compared with all vectors obtained from a calibration sequence (see Fig. 7) where each code level, d(0-31), is assigned the correspondent parity level, p(0-15). The color bits of the nearest calibration point are assigned to the time slot. A Euclidean metric is applied to measure the distances. We have tested the algorithm with different random sequences of the channels and we have recovered the original color bits, as shown in the top of Fig. 8.

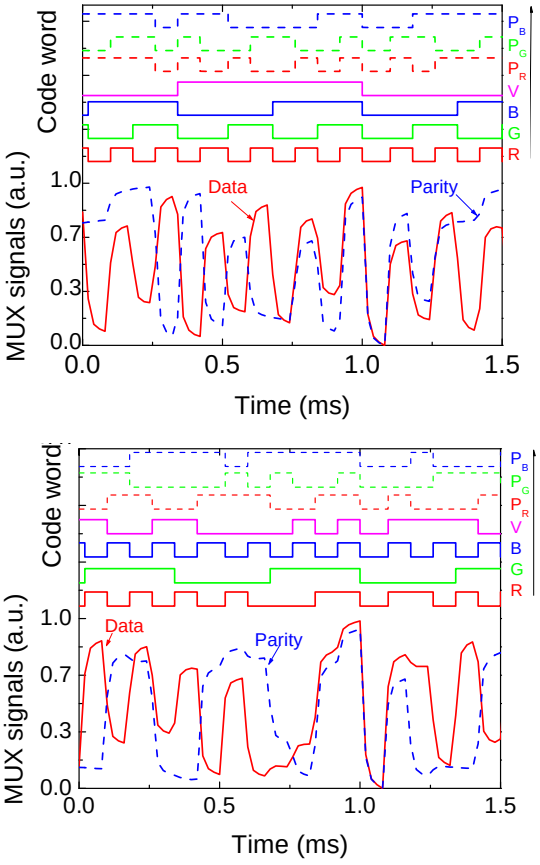

Fig. 8. Two different code and parity MUX/DEMUX signals under 390 nm front irradiation. On the top the transmitted channels are decoded.

4. Driving Distance

Lumens of light emitted by an LED depend on the current passing through the LED. For the luminous path loss (L_L), the conversion of the current flowing through the LED to lumens is given by [16].

$$L_L = \frac{1}{D^2} \times (\text{emitted power of the LED}), \quad (4)$$

where D is the distance between the LED and the receiver. The light generated by an LED is directly proportional to the forward current flowing through the device. In order to analyze the influence of white LED brightness (headlight-like) on the sensor response, the drive current applied to each chip was changed, keeping all the same level for equal white

perception. The intensity of the violet LED was kept constant at 30 mA. Each chip was modulated as shown on the top of Fig. 7. In Fig. 9(a), the MUX signal is displayed for different applied drive currents. In Fig. 9(b), the [1111] code level magnitudes, d_{15}, (arrow in Fig. 9(a) as a function of the drive current is displayed. The dotted curve shows the trend of the photocurrent with the relative distance from the receiver to the transmitter. Experimental results show that as the drive current increases, the intensity of the MUX signal also increases, but its shape remains the same. The sixteen levels, each one ascribed to an *on/off* possible state, are all detected allowing at the receiver the demultiplexing operation and the recovery of the transmitted information. Fig. 9(b), also shows that the code levels magnitude increases in a fast rate up to driving currents around 10 mA and then the photocurrent keeps increasing with the driving current but at a slow rate. Here, if we plot the photocurrent as a function of the one over the square of the driving current (dot plot) we can map the relative distances between the receiver and the transmitter. If the irradiance is calibrated for a known separation between the transmitter and the receiver, the irradiance at a given distance can be calculated using the inverse square law, hence, as the photocurrent increases the relative distance decreases exponentially. Three regions are detected: region A where the photocurrent decreases slowly with the distance; region B where its decrease is gradual; and region C, where a fast decrease occurs. These three regions can be directly correlated with the inter-vehicle driving distance from Fig. 2, after a calibration. So, by measuring the photocurrent at fixed code level it enables the prediction of the distance between vehicles and provides information to warn the driver about the safety distance (Fig. 2). This warning can be transmitted through one of the four available channels.

The VLC system compares the three received messages and infers the driving distance between the leader and the follower vehicles by reading the magnitude of the higher level (dash dot arrow in the figure) in the middle sensor. A warning message should be sent if the distance is lower than the safety distance.

We have simulated the scenario B (Fig. 2). The drive current applied to the two LEDs (headlamps-like) was the same and adjusted in order to have the same lighting conditions of this region. Here, the right and the left sensor receive the same message and the one in the middle receives the overlap of both. We have applied to the RGB LED a current of the order of 4 mA and 30 mA to the violet one.

In Fig. 10, the received MUX signals on the right and left sensors or in the middle one are displayed.

The solid lines are ascribed to the MUX data word and the dotted lines to the correspondent parity MUX. The same 4:3 binary information (on the top of the figure) was sent simultaneously by both LEDs.

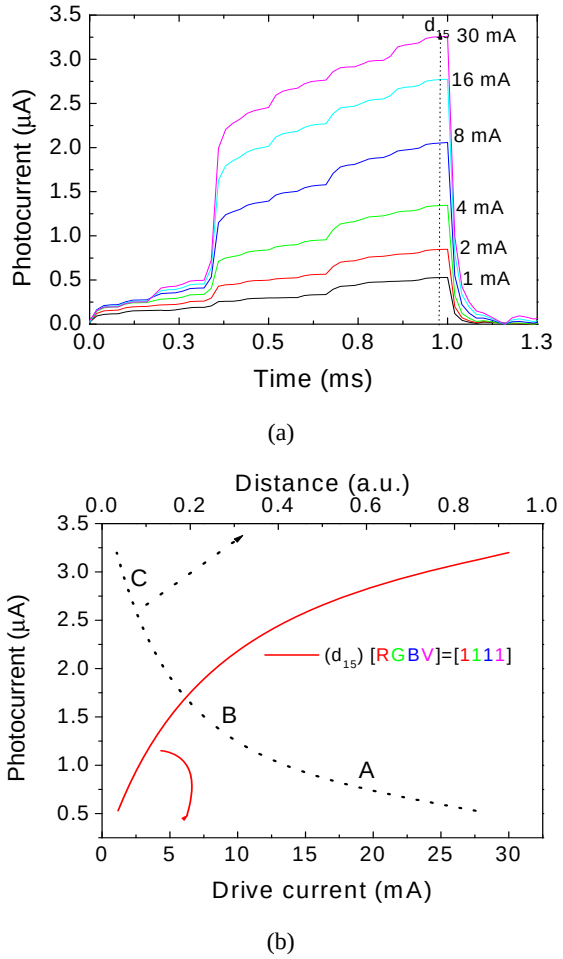

Fig. 9. (a) MUX signal under different drive currents applied to the chips of the trichromatic LED. (b) [1111] code level magnitude as a function of the drive current applied to the RGB chips.

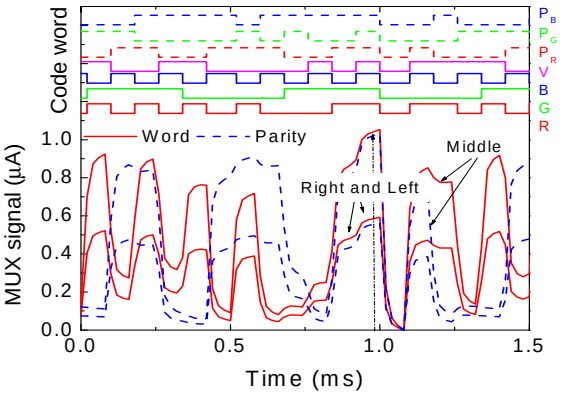

Fig. 10. MUX (solid line) and parity (dotted line) signals acquired by the right, the left and the middle receivers.

As expected, the shape of both code and parity MUX signals are the same but the intensity in the middle sensor (≅1 μA) is almost twice of the one received in the two others (≅0.5 μA).

Note that, when applying to each chip a forward current of the order of 4 mA, the magnitude of the data MUX signal is ≅1 μA (Fig. 9 (b) to which

corresponds a relative distance around 0.4 that leads to region B.

5. I2V and V2V Hybrid Communication

The introduction of individual vehicle location data via connected vehicles allows the development of new types of mobility applications.

The VLC applications for vehicular communication fall into two categories: Infrastructure-to-Vehicle (I2V) and Vehicle-to-Vehicle (V2V). For the I2V applications they focus on utilizing the traffic related infrastructure, such as traffic light or street light to communicate useful information. There are two types of transmitters in V2I communications. In the first type, the street lights whose primary purpose is to provide illumination can be used for data communication with cars or pedestrians. The second type are traffic lights based on LEDs that can also communicate with cars, if modulated. Since their primary purpose is not illumination and because they are always ON (even when there is sunlight), they are suitable for applications such as vehicle safety, traffic information broadcast, etc. On the other hand, the illumination LEDs are available on streets even where there are no traffic lights, making them more suitable for Internet access and positioning.

An Infrastructure to Vehicle (I2V) follow by Vehicle to Vehicle (V2V) communication was simulated and its architecture displayed in Fig. 11. The street light sends a coded message (traffic message) that includes its ID (violet channel) and traffic information (RGB channels). Each lamp transmits data during the time slot it occupies, i.e., the individual LED lamp transmits its own data depending on the area it locates. This message is received and decoded by the follower vehicle and retransmitted to the leader.

In the I2V communication, the emitter was developed based on street lights, located on roadside, and the transmitted information received and decoded in the SiC pinpin device, located in the car roof. The street lights emit light signals within a capture range across one or more road lanes. When a probe vehicle enters the street light´s capture range, the receivers in the probe vehicles respond to light signal and its unique ID and traffic message are assigned. They send a codeword message [RGBV: P_R, P_G, P_B] composed by red, green, blue and violet 4-binary bits (four input data bits [R G B V]) and generate three additional parity bits [P_R, P_G, P_B] for easy decoding and error control [10].

To build the V2V system that allows feedback channel between leader vehicle and follower vehicle, the follower vehicle sends the message that is received by the leader and can be retransmitted for the next car [17].

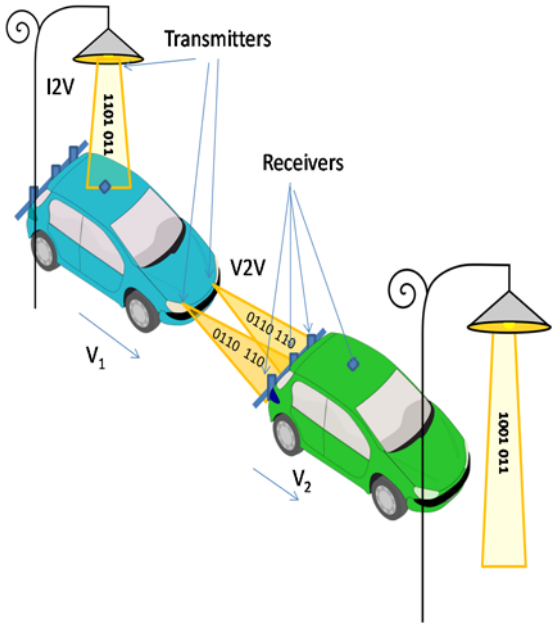

Fig. 11. Illustration of the proposed scenario: V2V and I2V hybrid systems.

In Fig. 12 the acquired MUX signals due to simulated an I2V communication follow by a V2V communication are presented.

In Fig. 12(a), the I2V MUX data (solid line) and parity (dash line) signals received by the roof sensor are displayed. In top the decoded signal is shown. In Fig. 12(b), the V2V MUX signals received on the right (R) and left (L) sensors or in the middle (M) one is displayed. The solid lines are ascribed to the MUX data word and the dash lines, to the correspondent parity MUX. The same 4:3 binary information (on the top of the figure) was sent simultaneously by both LEDs. Here, we have simulated the scenario B (see Fig. 2), the drive current applied to the two RGB-LEDs (headlamps-like) was the same and adjusted in order to have the same lighting conditions of this region. Experiments were conducted on straight and not on turning and zigzag paths.

Results (Fig. 12(a) show that in the analyzed time slot, the street light send a code message that is received at the pinpin sensor located at the car roof (MUX signal, I2V data) and decoded (RGBV:$P_RP_GP_B$). This message is transmitted to the headlights and send to the leader vehicle (Fig. 12(b). Here the right and the left sensor receive the same message and the one in the middle receives the overlap of both. We have applied to the RGB LED a current of the order of 4 mA and 30 mA to the violet one. As expected, the shape of both code and parity MUX signals are the same but the intensity in the middle sensor (≅1 μA) is almost twice of the one received in the two others (≅0.5 μA).

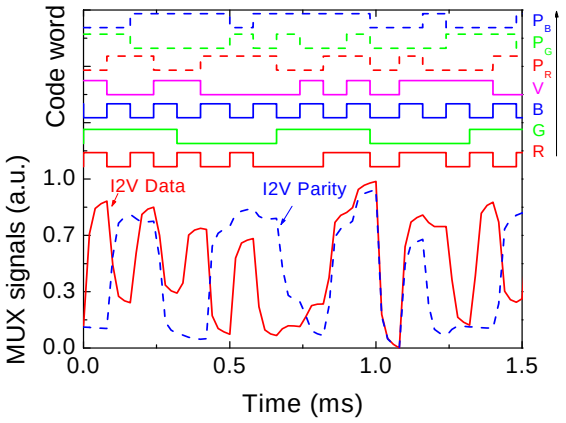

(a)

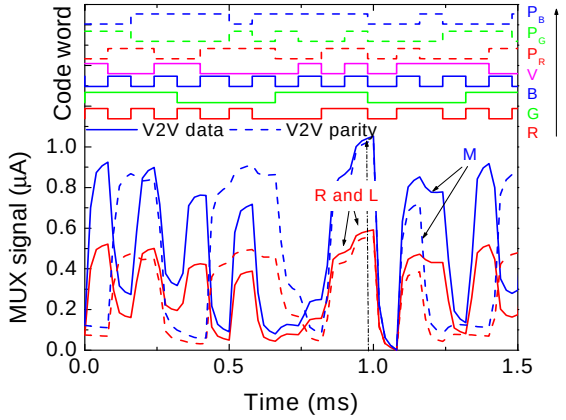

(b)

Fig. 12. Proof of concept: (a) Signals acquired in a I2V communication, MUX (solid line) and parity (dash line) signals; (b) Signals acquired by the R (right); L (Left); and M (middle) receivers in a V2V communication, MUX (solid line) and parity (dash line) signals.

5. Conclusion

In this paper, a VLC system, for vehicle safety applications, was presented. The system is composed of a VLC transmitter that modulates the light produced by white RGB-LEDs, and by VLC receivers based on photosensitive elements (a-SiC:H pinpin photodiodes) that code and decode the modulated signals. A scenario for the VLC system was tested and analyzed and a traffic scenario was simulated. By reading out in the receivers the magnitude of the multiplexed signal, it was possible, concurrently, to decode a transmitted message and to infer the driving distance between the transmitter and the receiver.

Acknowledgements

This work was sponsored by FCT – Fundação para a Ciência e a Tecnologia, within the Research Unit CTS – Center of Technology and systems, reference UID/EEA/00066/2013 and by the IPL project VLC_MIMO, 2016 and IPL/2017/SMART_VeDa/ISEL

References

[1]. S. Yousefi, E. Altman, R. El-Azouzi, Fathy, M., Analytical model for connectivity in vehicular Ad Hoc networks, *IEEE Transactions on Vehicular Technology*, Vol. 57, No. 6, 2008, pp. 3341-3356.

[2]. N. Kumar, N. Lourenço, D. Terra, L. N. Alves, R. L. Aguiar, Visible Light Communications in intelligent transportation systems, in *Proceedings of the IEEE Intelligent Vehicles Symposium*, 2012, pp. 748-753.

[3]. C. Liu, B. Sadeghi, E. W. Knightly, Enabling vehicular visible light communication (V2LC) networks, in *Proceedings of the Eighth ACM International Workshop on Vehicular Inter-networking (VANET'11), ACM*, New York, NY, USA, 2011, pp. 41-50.

[4]. P. Papadimitratos, A. La Fortelle, K. Evenssen, R. Brignolo, S. Cosenza, Vehicular communication systems: Enabling technologies, applications, and future outlook on intelligent transportation, *IEEE Communications Magazine*, Vol. 47, No. 11, November 2009, pp. 84-95.

[5]. S. Schmid, G. Corbellini, S. Mangold, T. R. Gross, An LED-to-LED Visible Light Communication system with software-based synchronization, in *Proceedings of the IEEE Globecom Workshops*, 2012,
pp. 1264–1268.

[6]. D. O'Brien, H. L. Minh, L. Zeng, G. Faulkner, K. Lee, D. Jung, Y. Oh, E. T. Won, Indoor visible light communications: challenges and prospects, in *Proceedings SPIE 7091*, 2008, pp. 709106-1 – 709106-9.

[7]. M. Vieira, P. Louro, M. Fernandes, M. A. Vieira, A. Fantoni, J. Costa, Three transducers embedded into one single SiC photodetector: LSP direct image sensor, optical amplifier and Demux device, *Advances in Photodiodes InTech*, Chap. 19, 2011, pp. 403-425.

[8]. M. A. Vieira, P. Louro, M. Vieira, A. Fantoni, A. Steiger-Garção, Light-activated amplification in Si-C tandem devices: A capacitive active filter model, *IEEE Sensor Jornal*, Vol. 12, No. 6, 2012, pp. 1755-1762.

[9]. I. L. Azevedo, M. G. Morgan, F. Morgan, The transition to solid-state lighting, in *Proceedings of the IEEE*, Vol. 97, No. 3, March 2009, pp. 481-510.

[10]. M. A. Vieira, M. Vieira, P. Louro, V. Silva, Error detection on a spectral data using an optical processor based on a-SiC technology, *Sensors & Transducers*, Vol. 184, Issue 1, January 2015, pp. 116-122.

[11]. R. W. Hamming, Error detecting and error correcting codes, *Bell Syst. Tech. J.*, Vol. 29, No. 2, 1960, pp. 147-160.

[12]. M. A. Vieira, M. Vieira, V. Silva, P. Louro, J. Costa, Optical signal processing for data error detection and correction using a-SiCH technology, *Phys. Status Solidi C*, Vol. 12, No. 12, 2015, pp. 1393–1400.

[13]. M. Vieira, M. A. Vieira, P. Louro, J. Costa, M. Fernandes, A. Fantoni, M. Barata, Multilayer architectures based on a-SiC:H material; Tunable wavelength filters in optical processing devices, *J. Nanosci. Nanotechnol.*, Vol. 11, No.6, 2011, pp. 5299-5304.

[14]. M. A. Vieira, M. Vieira, V. Silva, P. Louro, M. Barata, Optoelectronic logic functions using optical bias controlled SiC multilayer devices, *MRS Proceedings*, Vol. 1536, 2013, pp. 91-96.
[15]. M. A. Vieira, M. Vieira, P. Louro, V. Silva, J. Costa, A. Fantoni, SiC multilayer structures as light controlled photonic active filters, *Plasmonics*, Vol. 8, No. 1, 2013, pp. 63-70.
[16]. I. Raza, S. Jabeen, S. R. Chaudhry, S. A. Hussain, M. S. Bhatti, M. H. Raza, Optical wireless channel characterization for indoor Visible Light Communication, *Indian Journal of Science and Technology*, Vol. 8, No. 22, 2015, pp. 1-9.
[17]. M. A. Vieira, M. Vieira, P. Louro, P. Vieira, Smart Vehicle Lighting System in the Visible Range: Vehicle-to-Vehicle Communication, in *Proceedings of the Eighth International Conference on Sensor Device Technologies and Applications (SENSORDEVICES'17)*, Rome, Italy, 10-14 September, 2017, pp. 57-62.

Published by International Frequency Sensor Association (IFSA) Publishing, S. L., 2017 (http://www.sensorsportal.com).

Norbert Lauinger

IFSA

The Human Eye:
an Intelligent Optical Sensor
(The Inverted Human Retina: a Diffractive-optical Correlator)

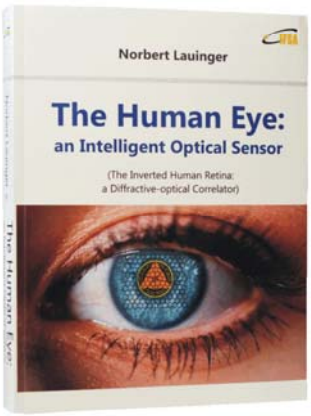

Hardcover: ISBN 978-84-617-2934-0
e-Book: ISBN 978-84-617-2955-5

The Human Eye: an intelligent optical sensor (The inverted retina: a diffractive - optical correlator) shows that the human eye from the prenatal structuring of the inverted retina hardware on up to the design of the central cortical visual pathway is not only different from but also radically more intelligent than a camera.

Many paradoxes in color vision (RGB peak positioning in the visible spectrum, overlapping of the RGB channels, relating local color to the whole scene, paradoxically colored shadows, Purkinje phenomenon etc.) are becoming intelligent solutions.

A fascinating book for all those wondering that the brightness of a scene is not cut in half and that the visible world doesn't collapse into a flat 2D-image when closing one eye. It should be a great of interest for students, scientists and engineers in eye-, vision- and brain-research, neuroscience, psychophysics, ophthalmology, psychology, optical sensor and diffractive optical engineering. Practical applications are the search for a retinal implant of the next generation and a helpful strategy against myopia in early childhood.

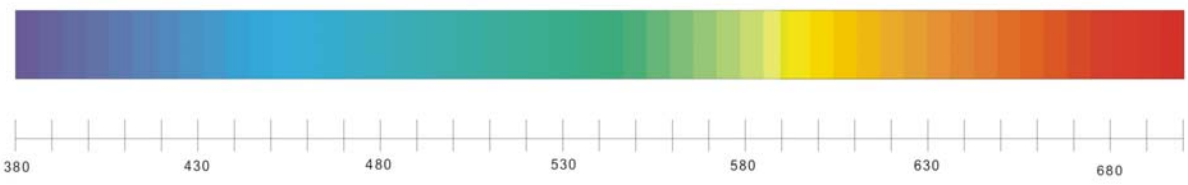

Order: http://www.sensorsportal.com/HTML/BOOKSTORE/Human_Eye.htm